JCTC Journal of Chemical Theory and Computation

Article

pubs.acs.org/JCTC

Application of Diffusion Monte Carlo to Materials Dominated by van der Waals Interactions

Anouar Benali,*[,†] Luke Shulenburger,*[,‡] Nichols A. Romero,*[,†] Jeongnim Kim,*[,§] and O. Anatole von Lilienfeld*[,†,∥]

[†]Argonne Leadership Computing Facility, Argonne National Laboratory, Argonne, Illinois 60439, United States

[‡]HEDP Theory Department, Sandia National Laboratories, Albuquerque, New Mexico 87185, United States

[§]Materials Science and Technology Division and Computer Science and Mathematics Division, Oak Ridge National Laboratory, Oak Ridge, Tenessee 37831, United States

[∥]Institute of Physical Chemistry, Department of Chemistry, University of Basel, Klingelbergstrasse 80, CH-4056 Basel, Switzerland

ABSTRACT: van der Waals forces are notoriously difficult to account for from first principles. We have performed extensive calculations to assess the usefulness and validity of diffusion quantum Monte Carlo when predicting van der Waals forces. We present converged results for noble gas solids and clusters, archetypical van der Waals dominated systems, as well as the highly relevant $\pi-\pi$ stacking supramolecular complex: DNA + intercalating anticancer drug ellipticine. Analysis of the calculated binding energies underscores the existence of significant interatomic many-body contributions.

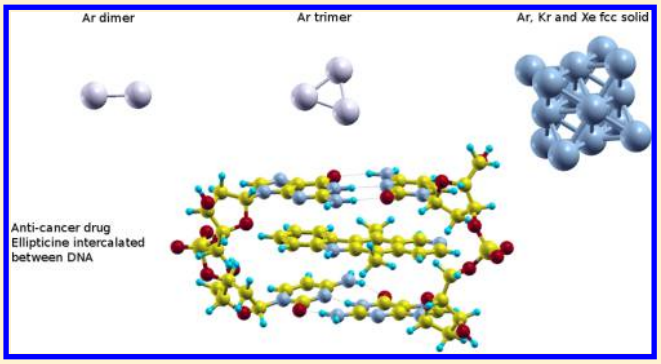

INTRODUCTION

The promise of virtual screening of molecules and materials for chemical or biological activity before experimental consideration relies on the ability to faithfully capture all the relevant physical interactions. Over the last decades, quantum chemistry simulations have enabled extensive studies of chemically diverse systems, using Hartree−Fock (HF) and post-HF methods as well as Density Functional Theory[1,2] (DFT). In principle, DFT could yield the exact potential energy and ground-state energy of any system if only the exchange and correlation (XC) potential in the Kohn−Sham Hamiltonian was known. In practice the XC potential must be approximated, and since the development of the first accurate local density and gradient corrected functionals, there has been an explosion in the number of available functionals.[3]

Unfortunately, many of these new functionals fail to accurately account for one of the most crucial phenomena in nature, namely, the noncovalent van der Waals (vdW) binding ubiquitous in any condensed material consisting of molecular subunits. At ambient conditions, for example, most liquids consist of molecules that do not evaporate due to their intermolecular vdW forces. As a result, many have proposed to correct the various XC-functionals through explicit inclusion of dispersion terms.[4−11] The simplest correction consists of adding a pairwise interatomic term decaying as C_6/R^6 to the potential obtained from DFT.[7,12−17] Such corrections show very promising results when employed for gas phase and small molecular dimers. However, for systems with charges or strong permanent multipole moments, the assumption of constant C_6-coefficients becomes problematic. For large systems, such as clusters, biomolecular polymers, or molecular crystals, one has to consider effects which go beyond the two-body London dispersion contributions. In particular, the many-body nature of vdW interactions[18−22] require the inclusion of Axilrod−Teller−Muto triple dipole[23,24] (decaying as C_9/R^9) as well as higher order terms.[25,26]

The HF method, on the other hand, yields all exchange interactions, however, it completely misses any dispersion interaction which is due to electron correlation. Post-HF methods, such as second-order Møller−Plesset perturbation theory (MP2)[27] provide a better approximation of the dispersion forces but are known for overestimating binding energies and underestimating equilibrium distances between molecules.[28] Chemical accuracy can be obtained, however, with methods such as coupled cluster theory with single, double and perturbative triple excitations, CCSD(T).[29] CCSD(T) has been the method of choice to create benchmark dispersion reference data for small molecular dimers.[30] More recently, it has also been used for solids.[31] The $O(N^7)$ computational complexity of this method, however, precludes its use for many or larger systems of general interest. Quantum Monte Carlo (QMC), and specifically diffusion Monte Carlo (DMC), represents a promising alternative to both the DFT as well as the post-HF approaches in that it retains high accuracy for both covalent and dispersion-dominated interactions while enjoying favorable

Received: April 15, 2014
Published: June 12, 2014

   dx.doi.org/10.1021/ct5003225 | J. Chem. Theory Comput. 2014, 10, 3417−3422

computational scaling of $O(N^3)$, equivalent to semilocal DFT. DMC treats the electron correlation explicitly and achieves high accuracy by solving the 3N-dimensional Schrödinger equation using stochastic sampling of the many-body green's function. As shown with recent calculations of first row dimers and the molecules in the G1 set,[32] or small molecular dimers,[33] subchemical accuracy can be obtained in QMC by systematically improving the nodal surface of the many-body wave function with an increasing number of determinants.

Moreover, the method's high scalability on petascale supercomputers has permitted its application to a wide variety of systems, from simple molecules to condensed phase metals.[34] In this paper, we demonstrate the usefulness of DMC's high accuracy and scalability for two large and complementary noncovalently bound systems. First, we analyze the dispersion interactions in noble gas cubic (FCC) crystals made of Ar, Kr, and Xe. Their cohesive energy being exclusively due to dispersion interactions, rare gas solids represent archetypical van der Waals systems, which are difficult to model at low pressures using uncorrected DFT (due to the inaccurate XC-potential) and very challenging using explicitly correlated electron/post-HF methods, due to their size and periodicity. We present and discuss DMC cohesive energy curves for rare gas solids. The predicted two- and three-body dispersion coefficients of Ar are validated by comparison to literature. Second, we have applied DMC to an isolated supramolecular complex. More specifically, we calculated the energy of interaction gained for intercalating the anticancer drug, ellipticine, in between two Watson−Crick base pairs held together by their respective sugar−phosphate DNA backbone. The binding between these moieties is biologically relevant for cancer treatment, and poses a significant computational challenge to any post-HF method. Our numbers are a first in terms of high-level ab initio computational predictions, and fill in important gaps of existing yet sparse experimental data.

METHODS

This study was performed using DMC within the fixed node approximation.[35] Since QMC, and more specifically, DMC, have been thoroughly reported,[36−38] we will only briefly describe the main features of our implementation in the QMCPACK package.[39−41]

To describe our systems, we used a single-determinant Slater−Jastrow wave function $\Psi(x_1,...,x_N)$ expressed as

$$\Psi(x_1, ..., x_N) = e^{J(\mathbf{x}_1,...,\mathbf{x}_N)}\Psi_{AS}(x_1, ..., x_N) \quad (1)$$

where $\mathbf{x}_i \equiv \{\mathbf{r}_i,\sigma_i\}$ is a space-spin coordinate, $J(\mathbf{x}_1,...,\mathbf{x}_N)$ is the Jastrow factor describing the correlation between electrons, $\Psi_{AS}(\mathbf{x}_1,...,\mathbf{x}_N)$ is the antisymmetric Fermionic part of the wave function and N is the total number of electrons.

The antisymmetric part is calculated within the framework of DFT, using the plane wave pseudopotential PWSCF code contained in the Quantum ESPRESSO (QE) simulation package.[42] The exchange and correlation energy-functional was modelled with the local density approximation (LDA) within the formulation proposed by Perdew and Zunger.[43] Convergence with respect to the kinetic energy cutoff (E_{cut}^{wfc}), the density cutoff (E_{cut}^{rho}), and the size of Monkhorst−Pack[44] mesh of k-points was checked for molecules and solids, in order to achieve the same precision in all calculations, leading to the following values: E_{cut}^{wfc} = 220 Ry, E_{cut}^{rho} = 880 Ry, and a (10 × 10 × 10) k-point grid in the FCC primitive cell for the bulk calculations. The single atom calculation and the molecule calculations were performed in cubic boxes with 30 au dimension ensuring an insignificant amount of interaction between atoms and their periodic images.

The Jastrow factor can be factored to one-body (effective electron−ion interactions), two-body (electron−electron interactions), three-body (electron−electron−ion interactions) and higher-body orders ($J = J_1J_2J_3$..). In this work, using one-body and two-body terms prove to be sufficient to describe accurately the electronic correlation.

$$J(r_1, ..., r_N) = \sum_{iI} \chi_i(r_{iI}) - \sum_{i<j} u(r_{ij}) \quad (2)$$

where χ and u are one-dimensional optimized splines. i labels the electron position, I labels the ion position, $r_{ij} = |\mathbf{r}_i - \mathbf{r}_j|$ is the electron−electron distance and $r_{iI} = |\mathbf{r}_i - \mathbf{R}_I|$ is the electron−ion distance. In this definition, χ is the cusp-less electron−Ion Jastrow factor, while u describes the spin independent electron−electron correlation. All the Jastrow parameters were optimized within the VMC correlated sampling framework[45] by minimizing a combination of the local energy E_L and the variance of the local energy. The Jastrow parameters, being all positive and multiplicative, and the nodes of the Slater−Jastrow wave function are determined by ψ_{AS}, and therefore, the fixed-node error in the DMC calculations is entirely due to the Slater determinant obtained from the DFT calculation.

All calculations were performed within the pseudopotential (PP) approximation, in which the core electrons are replaced by a nonlocal potential operator.[36] In the DMC part, we used the locality approximation[46] to evaluate the nonlocal PP. Norm-conserving pseudopotentials[47] (NCPP) were used for both QMC and DFT calculations. They were defined with ($3s^23p^6$) valence electrons for Argon atoms, ($4s^24p^6$) for Krypton atoms and ($4d^{10}5p^6$) for Xenon atoms and generated with the OPIUM[48] code and validated in a previous paper.[34] The orbitals were evaluated using real space cubic b-splines,[49] and we used 4096 walkers with a 0.01 au time step for the DMC calculations. For the molecular systems, the time step was extrapolated linearly to zero by also performing calculations at time steps of 0.012, 0.014, and 0.016. The time step error was quite small for these systems, being at largest 1.22 mHa/atom. For the case of the solids, the time step error was checked both at low and high pressure in a manner described in ref 34.

FINITE-SIZE EFFECTS: SOLIDS

An additional calculation when determining properties of solids in the thermodynamic limit with QMC using periodic boundary conditions is the necessity to control finite-size errors arising from the spurious correlations created by the periodic images of the system. These errors can be grouped into two categories, single-particle effects and many-body effects. In single-particle theories, calculations are usually reduced to the primitive unit cell. In single-particle theories (and effective single particle theories such as DFT), the properties of a system in the thermodynamic limit may be determined by using periodic boundary conditions and integrating over the first Brillouin zone. Although such an integration is possible in a many-body theory such as DMC, there is an additional finite-size error due to the additional symmetry and more sophisticated techniques are needed to extrapolate to the thermodynamic limit. For this reason, DMC

calculations of periodic solids are generally performed using supercells to minimize this error whereas DFT calculations may be performed in the primitive cell, resulting in a significant computational savings. A change in the twists changes the grid over which the kinetic energy is calculated. The solution is to use twist averaging (i.e., take the average of expectation values over all the k-points in the primitive cell). The error can therefore be reduced by increasing the density of the twist grid. A $2 \times 2 \times 2$ twist averaging is found to be sufficient for the 108-atom supercells used in this study.

When simulating systems with periodic boundary conditions, the sums over the infinite number of images do not converge when using the classical Coulomb potential. The common solution is to use the Ewald interaction.[50] However, the periodicity of the system implies the periodicity of the electronic correlations, introducing effects of electrons interacting with their periodic images in neighboring cells. This unphysical error corresponds to an XC energy of a system with a periodic XC hole. These errors are not present in DFT simulations since the XC interactions are derived from the electron gas converged at the limit of infinitely large simulation cells. The first finite-size correction consists of increasing the system size in order to reduce the spurious effective interactions between an electron and its XC hole. Supercells can be generated using the Bloch theorem by reproducing the wave function only in the primitive cell. Even if calculations on larger supercells are possible, it leads to a rapidly increasing cost of the calculations with the number of electrons in the simulation cell. The second finite-size correction is to add the model periodic Coulomb[51] (MPC) interaction to the Ewald energy as suggested by Fraser et al. The last correction is applied to the kinetic energy following the scheme of Chiesa[52] et al. For all calculations in this study, energy convergence was reached at simulation cells containing 108 atoms and applying both MPC and Chiesa corrections.

RESULTS AND DISCUSSION

Rare Gas Clusters. The DMC dispersion energy contribution of Ar atoms I in positions $\mathbf{R}_I$ can be used to investigate the many-body expansion of interatomic potentials. In the dissociation limit, or for neutral atoms with non-overlapping electron density, the leading order of the two-body dispersion contribution (dipole−dipole) to the energy corresponds to London's formula,[53,54]

$$E_{(2)}(\mathbf{R}_I, \mathbf{R}_J) = -\frac{C_{6_{IJ}}}{R_{IJ}^6} \tag{3}$$

while the leading order term of the three-body contribution (dipole−dipole−dipole) is given by Axilrod−Teller−Muto,[23,24]

$$E_{(3)}(\mathbf{R}_I, \mathbf{R}_J, \mathbf{R}_K) = C_{9_{IJK}} \frac{1 + 3\cos[\phi_i]\cos[\phi_j]\cos[\phi_k]}{(R_{IJ}R_{IK}R_{JK})^3} \tag{4}$$

where $R_{IJ} = |\mathbf{R}_I - \mathbf{R}_J|$ and $\{\phi_i\}$ are the interatomic distances and angles, respectively.

Here, the two-body and three-body interaction energies are defined as functions of the energies of monomer (E_{mon}), dimer (E_{dim}), and trimer (E_{trim}),

$$E_{(2)} = E_{\mathrm{dim}} - 2E_{\mathrm{mon}} \tag{5}$$

$$E_{(3)} = E_{\mathrm{trim}} - 3E_{(2)} - 3E_{\mathrm{mon}} \tag{6}$$

The DMC predictions for Ar's two- and three-body energies as a function of interatomic distance are shown in Figure 1, together with CCSD(T) and DFT results taken from the literature.[20,21,55] Note that only the equilateral triangle geometry is considered in the case of the trimer.

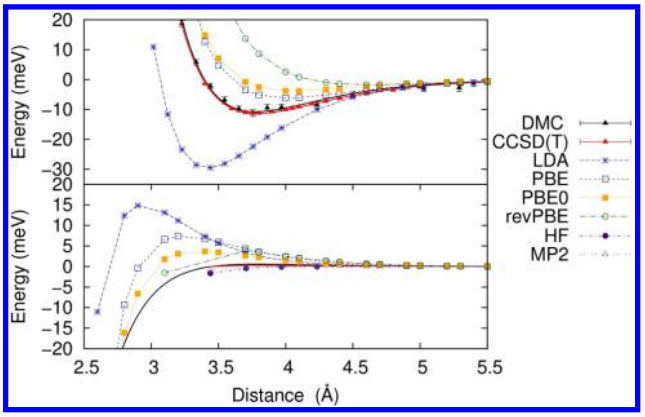

Figure 1. Interatomic two- and three-body potential energies [eqs 3 and 4] as a function of the interatomic distance for argon dimer (top) and trimer (bottom) using DMC, DFT results from ref 20 and CCSD(T), MP2 and HF-results from ref 55.

Using a Vinet fit[56] over the DMC energies, we see that QMC and CCSD(T)-energies are always within less than 0.1 meV for Ar dimer and trimer. To further quantify the agreement, we have fitted eqs 3 and 4 to estimate the leading order's dispersion coefficients of the DMC data. The resulting C_6 and C_9 coefficients, shown in Table 1, are in very good agreement

Table 1. London and Axilrod−Teller−Muto Dispersion Coefficients for Ar

level of theory	C_6	C_9
Hirshfeld[a]	64.3	518.0
TDDFT[b]	64.2	523.0
DFT-D3[b]	64.2	519.8
DMC[c]	63.1	517.6
Exp[d]	64.4	519.0

[a]Ref 21. [b]Ref.57. [c]This work. [d]Ref 58.

with data estimated in the literature, and experiment. We suspect the small remaining deviation to be due to the neglect of C_8, C_{10}, or C_9-contributions, present in the DMC results, yet absent in eqs 3−4).

Rare Gas Crystals. Encouraged by the accurate results for the Ar dimer and trimer, we have proceeded to use DMC for the study of rare gas crystals. Specifically, we have calculated the cohesive energy as a function of density for noble gas solids: Ar, Kr, and Xe. All calculations were done using a 108-atom supercell with $2 \times 2 \times 2$ twists and finite-size corrections. To obtain cohesive energy estimates, E_{coh}, we refer to the isolated atom energy estimate obtained from the Vinet[56] fit extrapolated to infinity. The resulting cohesive energy versus lattice constant curves, calculated with DMC for Ar, Kr and Xe, are displayed in Figure 2. We have also assessed the accuracy of the DMC results by comparison to precisely measured properties of the rare gas crystals. In Table 2, we compare the fitted values of equilibrium volume and bulk modulus with measured quantities from the literature. Overall, we note a very good agreement with experiments. In the case of Ar, the agreement is excellent

dx.doi.org/10.1021/ct5003225 | J. Chem. Theory Comput. 2014, 10, 3417−3422

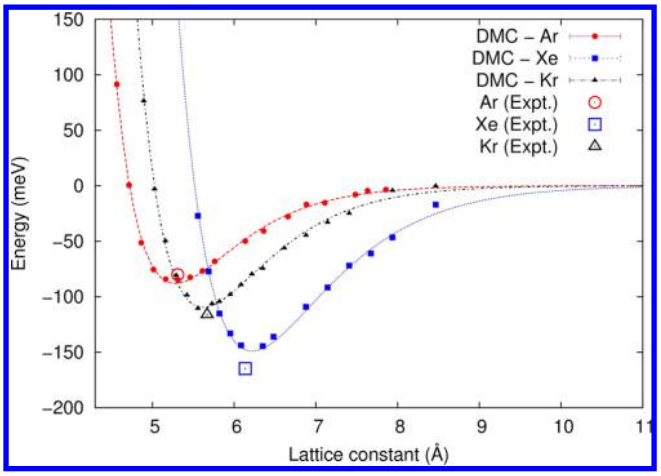

Figure 2. DMC ground-state total energies per atom of fcc Ar, Xe, and Kr crystals. All calculations were done using 108-atom supercell. Dashed lines correspond to the Vinet fit.[56]

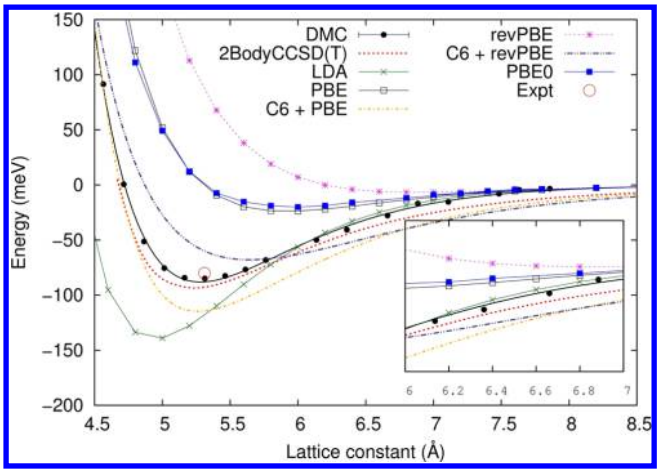

Figure 3. Cohesive energies of fcc Ar crystal for various levels of theory including our DMC numbers, DFT results from ref 20 and CCSD(T), MP2 and HF-results from ref 55.

for the cohesive energy and lattice constant. The DMC bulk modulus, however, is slightly overestimated, suggesting a slightly too stiff potential. For the Kr crystal, DMC underestimates the binding by more than 10 meV. However, excellent agreement can be found in terms of bulk modulus and lattice constant. DMC also underestimates the cohesive energy and the bulk modulus of Xe, by ∼20 meV and 0.4 GPa, respectively. Xenon's lattice constant is overestimated by ∼0.1 Å. The DMC-based prediction becomes increasingly challenging as one goes down the column in the periodic table. This increase in error might be due to the neglect of *d*-electrons through the use of pseudopotentials. For Xe, relativistic effects could also be at the origin of this observation. It is also worth noting that the very shallow and broad minima of the Kr and Xe crystals imply a strong sensitivity of the results to small errors in the DMC sampling.

Comparison of Ar Crystal. Due to readily available and abundant data, we have selected the Ar crystal for further analysis. In Figure 3, cohesive energies versus lattice constant are shown for various levels of theory, together with the experimental value, and our DMC results from Figure 2. The DMC curve accurately reproduces depth and location of the experimental value, obtained through subtraction of the zero-point energy (estimated in ref 61) from the measured cohesive energy, taken from ref 59. Summation of CCSD(T) two-body energies obtained for the isolated Ar dimers (ref 62) over all pairs of atoms in the crystal yields an estimated cohesive energy curve that is slightly below the DMC curve for the minimum region as well as in the dissociative tail. Corrected and uncorrected DFT results, taken from ref 20 are also shown in Figure 3, with LDA overestimating the binding and underestimating the equilibrium lattice constant, while the GGA (PBE, revPBE) and hybrid functionals (PBE0) underestimate the binding and overestimate the equilibrium lattice constant. It is interesting to note, however, that in the dissociation regime (lattice constant larger than 5 Å) all DFT methods converge onto a rapidly decaying, single-binding curve which closely resembles the DMC curve. By contrast, the two-body CCSD(T) curve, as well as the curves obtained from the two-body based C_6 corrections to PBE and revPBE, decay at a significantly slower rate. Assuming our DMC-level of theory for Ar to be sufficiently accurate, in particular also with respect to the aforementioned overestimated bulk modulus, this analysis suggests that there are considerable repulsive many-body interactions in the Ar crystal which dampen the two-body attraction, leading to a more rapidly decaying cohesive energy. Consequently, our results amount to additional and independent numerical evidence that correcting DFT functionals with only two-body interatomic terms, while correctly increasing the binding in the equilibrium region, simultaneously leads to an overestimation of the binding in the dissociative regime. As such, our findings are consistent with the conclusions of refs 20, 21, and 57.

Ellipticine Intercalation. The encouraging results and insights gained from the application of DMC to rare gas molecules and solids have motivated us to address the question if DMC yields similar performance for more complex systems, dominated by vdW interactions. The $\pi-\pi$-stacking dispersion interaction between molecular entities with permanent multipole-moments and large molecular polarizabilities represent a highly realistic and relevant scenario since this interaction corresponds to a major contribution in the structure of biomolecular systems, such as DNA.[14,62] In this context, we have have applied DMC to the binding of a small molecule to

Table 2. Diffusion Monte Carlo (DMC) and Experimental Results for Various Properties of fcc Ar, Kr, and Xe Solids[a]

fcc crystal	E_{coh} (meV)	$\sim E_{coh}^{exp}$ (meV)	B_0 (GPa)	B_0^{exp} (GPa)	a_0 (Å)	a_0^{exp} (Å)	χ^2
Ar	80.3 ± 1.0	80.1	3.3 ± 0.1	2.86	5.340 ± 0.014	5.311	3.24
Kr	103.8 ± 1.5	116.0	3.6 ± 0.1	3.34	5.655 ± 0.015	5.670	11.08
Xe	143.6 ± 1.4	164.7	3.2 ± 0.1	3.63	6.241 ± 0.006	6.132	4.85

[a]Experimental cohesive energies are from ref 59. Experimental lattice constants and bulk moduli are from ref 60. E_{coh}, B_0, and a_0 are the cohesive energy, bulk modulus, and equilibrium lattice constant, respectively. All values have been corrected taking into account zero-point motion of the atoms within the quasi-harmonic approximation. χ^2 refers to the χ-square test of the Vinet fit,[56] used to obtain a continuous potential curve.

dx.doi.org/10.1021/ct5003225 | J. Chem. Theory Comput. 2014, 10, 3417−3422

DNA through the mechanism of intercalation.[63] This mechanism has been observed for planar polycyclic aromatic molecules which, inserted between two consecutive base pairs of DNA, can be active in antitumor chemotherapy.[64] In general, the commonly polar and often charged intercalators bind to DNA by noncovalent $\pi-\pi$-stacking with the nucleic acid Watson−Crick base pairs, often combined with H-bonding to solvent. Leaving entropic effects aside, the relative free energy of binding will be significantly affected by the system's potential energy of interaction. The aromatic polycyclic systems exhibit strong polarizabilities resulting in dispersion energy being one of the major stabilizing components of the binding energy.

For this study, we have investigated the utility of DMC for describing such systems by calculating the binding energy of ellipticine to two Watson−Crick bonded cytosine−guanine base pairs linked by their respective phosphate sugar puckers, as depicted in Figure 4. Ellipticine is an alkaloid isolated from

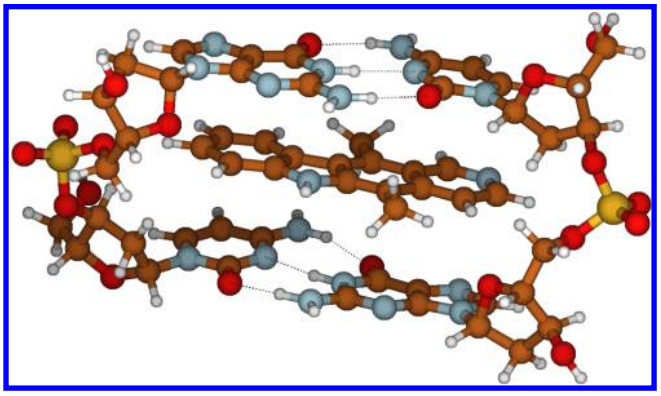

Figure 4. Ellipticine molecule (neutral) intercalated into two Watson−Crick bound DNA base-pairs, covalently bound through deprotonated sugar−phosphate backbone fragment.

apocyanaceae plants and several of its more soluble derivatives exhibit significant antitumor and anti-HIV activities.[65] The main reason for the interest in ellipticine and its derivatives for clinical purposes is due to their high efficencies against several types of cancer and their rather limited toxic side effects.[66] Ellipticine's mode of action is thought to be based mainly on DNA intercalation. Over the past decades, the binding of ellipticine to DNA has been investigated with multiple computational methods.[21,25,67,68] We find that DMC predicts a binding energy of −33.6 kcal/mol. In Table 3, this number is compared to previous literature results. DFT(PBE) without dispersion corrections fails qualitatively in describing the binding of ellipticine to DNA. When correcting DFT with two-body forces (DFT+C_6), then three-body forces (DFT +C_6+C_9), the binding energy difference to the DMC value is reduced to a few kcal/mol. However, corrections using an empirical Fermi-type damping function (vdW-TS)[69] or the DFT-MBD[70] using a range-separated Coulomb potential tend to overestimate the binding. The recently published revised DFT+MBDr method[71] yields, so far, the number that comes closest to the DMC result.

CONCLUSIONS

We have validated the application of DMC to systems dominated by dispersion interactions by performing extensive calculations of the binding of Ar atom dimers and trimers. The resulting dispersion coefficients are in excellent agreement with

Table 3. Binding Energies (ΔE_{bind}) [kcal/mol] for the DNA−Ellipticine Complex Depicted in Figure 4, Calculated Using Pure DFT (PBE), DFT with Ad Hoc Addition of Damped C_6 and C_9 Terms, DFT with Self-Consistent Screening and Two- (TBD) and Many-Body (MBD) Dispersion Corrections, and DFT with Dispersion Corrected Atom-Centered Potentials (DCACP)

level of theory	ΔE_{bind}
DFT(PBE)	+5.2
DFT+C_6	−46.9[a]
DFT+C_6+C_9	−37.0[a]
DFT+TBD	−39.1[b]
DFT+MBD	−50.7[b]
DFT+MBDr	−35.4[c]
DFT+DCACP	−37.0[d]
DMC	−33.6 ± 0.9

[a]Ref 21. [b]Ref 25. [c]Private communication from authors of ref 71. [d]Ref 67.

reference values from the literature. We have also found very good agreement with experimental values of the cohesive energy, bulk modulus, and lattice constants of Ar, Kr, and Xe fcc crystals. By comparing our Ar crystal DMC results to corresponding two-body-based cohesive energy estimates, we conclude that many-body interatomic contributions reduce the attraction in the dissociative tail of the crystal. Finally, we have shown that DMC can be applied directly to the study of large biomolecular assemblies which typically exceed the computational feasibility when treated with post-Hartree−Fock wave function methods, such as CCSD(T). As such, we conclude that DMC is a promising tool for providing valuable reference values for benchmarking and developing atomistic simulation methods for more extended systems with electronically challenging interaction regimes, as also very recently highlighted in ref 72. We expect DMC to become routinely useful in both the development and benchmarking of new approximate DFT techniques as well as interatomic potentials capable of accurate treatment of van der Waals systems. In the long term, such developments promise to enable the predictive routine simulation of large supra-molecular assemblies, molecular liquids and crystals.

AUTHOR INFORMATION

Corresponding Authors

*Email: benali@anl.gov.
*Email: lshulen@sandia.gov.
*Email: naromero@anl.gov.
*Email: jnkim@ornl.gov.
*Email: anatole.vonlilienfeld@unibas.ch.

Notes

The authors declare no competing financial interest.

ACKNOWLEDGMENTS

We thank the authors of ref 71 (A. Tkatchenko and A. Ambrosetti) for providing an MBDr value for the ellipticine binding (Table 3). This research used resources of the Argonne Leadership Computing Facility at Argonne National Laboratory, which is supported by the Office of Science of the U.S. Department of Energy under contract DE-AC02-06CH11357. This work was done, in part, under the ALCF-2 Early Science Program. Sandia National Laboratories is a multiprogram laboratory managed and operated by Sandia Corporation, a

wholly owned subsidiary of Lockheed Martin Corporation, for the U.S. Department of Energy's National Nuclear Security Administration under Contract No. DE-AC04-94AL85000. O.A.v.L. acknowledges funding from the Swiss National Science foundation (No. PPOOP2_ 138932). L.S., N.A.R., and J.K. are supported through Predictive Theory and Modeling for Materials and Chemical Science program by the Basic Energy Science (BES), Department of Energy (DOE).

REFERENCES

(1) Hohenberg, P.; Kohn, W. *Phys. Rev.* **1964**, *136*, B864−B871.
(2) Kohn, W.; Sham, L. J. *Phys. Rev.* **1965**, *140*, A1133−A1138.
(3) Staroverov, V. N.; Scuseria, G. E.; Tao, J.; Perdew, J. P. *Phys. Rev. B* **2004**, *69*, 075102.
(4) Lin, I.-C.; Coutinho-Neto, M. D.; Felsenheimer, C.; von Lilienfeld, O. A.; Tavernelli, I.; Rothlisberger, U. *Phys. Rev. B* **2007**, *75*, 205131.
(5) Dion, M.; Rydberg, H.; Schröder, E.; Langreth, D. C.; Lundqvist, B. I. *Phys. Rev. Lett.* **2004**, *92*, 246401.
(6) Wu, Q.; Yang, W. *J. Chem. Phys.* **2002**, *116*, 515−524.
(7) Grimme, S. *J. Comput. Chem.* **2004**, *25*, 1463−1473.
(8) von Lilienfeld, O. A.; Tavernelli, I.; Rothlisberger, U.; Sebastiani, D. *Phys. Rev. Lett.* **2004**, *93*, 153004.
(9) Silvestrelli, P. L. *Phys. Rev. Lett.* **2008**, *100*, 053002.
(10) Tkatchenko, A.; Scheffler, M. *Phys. Rev. Lett.* **2009**, *102*, 073005.
(11) Torres, E.; DiLabio, G. A. *J. Phys. Chem. Lett.* **2012**, *3*, 1738−1744.
(12) LeSar, R. *J. Phys. Chem.* **1984**, *88*, 4272−4278.
(13) Meijer, E. J.; Sprik, M. *J. Chem. Phys.* **1996**, *105*, 8684.
(14) Elstner, M.; Hobza, P.; Frauenheim, T.; Suhai, S.; Kaxiras, E. *J. Chem. Phys.* **2001**, *114*, 5149−5155.
(15) Wu, X.; Vargas, M. C.; Nayak, S.; Lotrich, V.; Scoles, G. *J. Chem. Phys.* **2001**, *115*, 8748−8757.
(16) Wu, Q.; Yang, W. *J. Chem. Phys.* **2002**, *116*, 515−524.
(17) Sánchez-Portal, D.; Ordejón, P.; Artacho, E.; Soler, J. M. *Int. J. Quantum Chem.* **1997**, *65*, 453−461.
(18) Bade, W. L. *J. Chem. Phys.* **1957**, *27*, 1280−1284.
(19) Donchev, A. G. *J. Chem. Phys.* **2006**, *125*, 074713.
(20) Tkatchenko, A.; von Lilienfeld, O. A. *Phys. Rev. B* **2008**, *78*, 045116.
(21) von Lilienfeld, O. A.; Tkatchenko, A. *J. Chem. Phys.* **2010**, *132*, 234109.
(22) Shtogun, Y. V.; Woods, L. M. *J. Phys. Chem. Lett.* **2010**, *1*, 1356−1362.
(23) Axilrod, B. M.; Teller, E. *J. Chem. Phys.* **1943**, *11*, 299−300.
(24) Muto, Y. *J. Phys. Math. Soc. Jpn.* **1943**, *17*, 629.
(25) DiStasio, R. A.; von Lilienfeld, O. A.; Tkatchenko, A. *Proc. Natl. Acad. Sci. U.S.A.* **2012**, *109*, 14791−14795.
(26) de-la Roza, A. O.; Johnson, E. R. *J. Chem. Phys.* **2013**, *138*, 054103.
(27) Møller, C.; Plesset, M. S. *Phys. Rev.* **1934**, *46*, 618−622.
(28) Tsuzuki, S.; Honda, K.; Uchimaru, T.; Mikami, M. *J. Chem. Phys.* **2004**, *120*, 647−659.
(29) Raghavachari, K.; Trucks, G. W.; Pople, J. A.; Head-Gordon, M. *Chem. Phys. Lett.* **1989**, *157*, 479−483.
(30) Jurecka, P.; Sponer, J.; Cerny, J.; Hobza, P. *Phys. Chem. Chem. Phys.* **2006**, *8*, 1985−1993.
(31) Booth, G. H.; Grüneis, A.; Kresse, G.; Alavi, A. *Nature* **2013**, *493*, 365−370.
(32) Morales, M. A.; McMinis, J.; Clark, B. K.; Kim, J.; Scuseria, G. E. *J. Chem. Theory Comput.* **2012**, *8*, 2181−2188.
(33) Dubecký, M.; Jurecka, P.; Derian, R.; Hobza, P.; Otyepka, M.; Mitas, L. *J. Chem. Theory Comput.* **2013**, *9*, 4287−4292.
(34) Shulenburger, L.; Mattsson, T. R. *Phys. Rev. B* **2013**, *88*, 245117.
(35) Reynolds, P. J.; Ceperley, D. M.; Alder, B. J.; Lester, W. A. *J. Chem. Phys.* **1982**, *77*, 5593−5603.
(36) Foulkes, W. M. C.; Mitas, L.; Needs, R. J.; Rajagopal, G. *Rev. Mod. Phys.* **2001**, *73*, 33−83.
(37) Umrigar, C. J.; Nightingale, M. P.; Runge, K. J. *J. Chem. Phys.* **1993**, *99*, 2865−2890.
(38) Hammond, B.; Lester, W.; Reynolds, P. *Monte Carlo Methods in Ab Initio Quantum Chemistry*; World Scientic: London, 1994.
(39) Kim, J.; Esler, K. P.; McMinis, J.; Morales, M. A.; Clark, B. K.; Shulenburger, L.; Ceperley, D. M. *J. Phys.: Conf. Ser.* **2012**, *402*, 012008.
(40) Kim, J.; Esler, K.; McMinis, J.; Ceperley, D. M. Quantum Monte Carlo algorithms: Making most of large-scale multi/many-core clusters. *Proceedings of the 2010 Scientific Discovery through Advanced Computing (SciDac) Conference*, Chattanooga, TN, July 11−15, 2010.
(41) Esler, K.; Kim, J.; Shulenburger, L.; Ceperley, D. *Comput. Sci. Eng.* **2012**, *14*, 40−51.
(42) Giannozzi, P.; et al. *J. Phys.* **2009**, *29*, 395502.
(43) Perdew, J. P.; Zunger, A. *Phys. Rev. B* **1981**, *23*, 5048−5079.
(44) Monkhorst, H. J.; Pack, J. D. *Phys. Rev. B* **1976**, *13*, 5188−5192.
(45) Umrigar, C. J.; Wilson, K. G.; Wilkins, J. W. *Phys. Rev. Lett.* **1988**, *60*, 1719−1722.
(46) Mitáš, L.; Shirley, E. L.; Ceperley, D. M. *J. Chem. Phys.* **1991**, *95*, 3467−3475.
(47) Hamann, D. R.; Schlüter, M.; Chiang, C. *Phys. Rev. Lett.* **1979**, *43*, 1494−1497.
(48) Walter, E. J. Opium Pseuopotential Generation Project, Version 3.7; http://opium.sourceforge.net (accessed 2013).
(49) Williamson, A. J.; Hood, R. Q.; Grossman, J. C. *Phys. Rev. Lett.* **2001**, *87*, 246406.
(50) Ewald, P. P. *Ann. Phys.* **1921**, *369*, 253−287.
(51) Fraser, L. M.; Foulkes, W. M. C.; Rajagopal, G.; Needs, R. J.; Kenny, S. D.; Williamson, A. J. *Phys. Rev. B* **1996**, *53*, 1814−1832.
(52) Chiesa, S.; Ceperley, D. M.; Martin, R. M.; Holzmann, M. *Phys. Rev. Lett.* **2006**, *97*, 076404.
(53) Heitler, W.; London, F. *Z. Phys.* **1927**, *44*, 455.
(54) Eisenschitz, R.; London, F. *Z. Phys.* **1930**, *60*, 491.
(55) Podeszwa, R.; Szalewicz, K. *J. Chem. Phys.* **2007**, *126*, 194101.
(56) Vinet, P.; Ferrante, J.; Smith, J. R.; Rose, J. H. *J. Phys. C: Solid State Phys.* **1986**, *19*, L467.
(57) Grimme, S.; Antony, J.; Ehrlich, S.; Krieg, H. *J. Chem. Phys.* **2010**, *132*, 154104.
(58) Herman, P. R.; LaRocque, P. E.; B. P. Stoicheff, B. P. *J. Chem. Phys.* **1988**, *89*, 4535.
(59) Schwalbe, L. A.; Crawford, R. K.; Chen, H. H.; Aziz, R. A. *J. Chem. Phys.* **1977**, *66*, 4493.
(60) Anderson, M.; Swenson, C. *J. Phys. Chem. Solids* **1975**, *36*, 145−162.
(61) Rościszewski, K.; Paulus, B.; Fulde, P.; Stoll, H. *Phys. Rev. B* **2000**, *62*, 5482.
(62) Slavicek, P.; Kalus, R.; Paska, P.; Odvarkova, I.; Hobza, P.; Malijevsky, A. *J. Chem. Phys.* **2003**, *119*, 2102.
(63) Reha, D.; Kabelac, M.; Ryjacek, F.; Sponer, J.; Sponer, J. E.; Elstner, M.; Suhai, S.; Hobza, P. *J. Am. Chem. Soc.* **2002**, *124*, 3366−3376, PMID: 11916422.
(64) Waring, M. J.; Bailly, C. *J. Mol. Recognit.* **1994**, *7*, 109−122.
(65) Poljakova, J.; Eckschlager, T.; Hrebackova, J.; Hrabeta, J.; Stiborova, M. *Biochem. Pharmacol.* **2001**, 1675.
(66) Auclair, C. *Arch. Biochem. Biophys.* **1987**, *1*, 1−14.
(67) Lin, I.-C.; von Lilienfeld, O. A.; Coutinho-Neto, M. D.; Tavernelli, I.; Rothlisberger, U. *J. Phys. Chem. B* **2007**, *111*, 14346−14354.
(68) Kolar, M.; Kubar, T.; Hobza, P. *J. Phys. Chem. B* **2010**, *114*, 13446.
(69) Tkatchenko, A.; Scheffler, M. *Phys. Rev. Lett.* **2009**, *102*, 073005.
(70) Tkatchenko, A.; DiStasio, R. A.; Car, R.; Scheffler, M. *Phys. Rev. Lett.* **2012**, *108*, 236402.
(71) Ambrosetti, A.; Reilly, A. M.; DiStasio, R. A.; Tkatchenko, A. *J. Chem. Phys.* **2014**, *140*, 18A508.
(72) Ambrosetti, A.; Alfè, D.; DiStasio, R. A.; Tkatchenko, A. *J. Phys. Chem. Lett.* **2014**, *5*, 849−855.